



Research article

Isolation, characterization and pharmacological potentials of methanol extract of *Cassia fistula* leaves: Evidenced from mice model along with molecular docking analysis

Mohammad Abdullah Taher^{a,e,*}, Aysha Akter Laboni^a, Md Ashraful Islam^b,
Hasin Hasnat^b, Mohammad Mahmudul Hasan^c, Jannatul Ferdous^d,
Suriya Akter Shompa^b, Mala Khan^{a,**}

^a Bangladesh Reference Institute for Chemical Measurements (BRiCM), Laboratory Road, Dhaka, 1205, Bangladesh

^b Department of Pharmacy, State University of Bangladesh, Dhaka, Bangladesh

^c Department of Chemistry, University of Dhaka, Bangladesh

^d Department of Statistics, University of Dhaka, Bangladesh

^e Department of Pharmaceutical Chemistry, Faculty of Pharmacy, University of Dhaka, Bangladesh

ARTICLE INFO

Keywords:

Phytochemistry
GC-MS/MS
FTIR
Analgesic
Hypoglycemic
Molecular docking

ABSTRACT

The purpose of the current investigation was to conduct a detailed analysis of the chemical components and medicinal properties of the methanolic crude extract derived from the leaves of *Cassia fistula*. This analysis was carried out using both experimental (in vivo) and computational (in silico) methods. Eleven chemicals were chromatographically isolated using GC-MS/MS, which utilizes a library of NIST and Wiley 2020 versions. FTIR analysis of the extract was performed to identify the functional group of the compounds. The glucose-lowering capacity, analgesic, and anti-diarrheal activities of methanolic crude extract were analyzed utilizing a well-known oral glucose tolerance test, tail immersion method, writhing assay, and castor oil-induced diarrheal mice methods, respectively. After 60 min, 120 min, and 180 min of loading the drugs, a significant reduction of blood glucose levels was examined ($p < 0.05$) in all the extracts of this plant (200 mg/kg, 400 mg/kg and 600 mg/kg) utilized in this research at a time-dependent manner. Similarly, all the crude extracts showed significant ($p < 0.05$) effects against pain centrally and peripherally compared to the standard drug morphine (2 mg/kg bw) and diclofenac sodium (50 mg/kg bw). Moreover, the methanol extract (400 mg/kg bw) manifested anti-diarrheal efficacy by inhibiting 72.0 % of the diarrheal episode in mice compared to the standard drug loperamide (inhibition = 80.0%). The results of the computational investigations corroborated existing in-vivo findings. Greater or close to equivalent binding affinity to the active binding sites of kappa opioid receptor, glucose transporter 3 (GLUT 3), and cyclooxygenase 2 was indicative of the potential anti-diarrheal, hypoglycemic, and analgesic characteristics of the isolated compounds (COX-2). Moreover, anticancer and antimicrobial potentiality was also found impressive through evaluation of binding affinity with epidermal growth factor receptor (EGFR) and dihydrofolate reductase (DHFR) receptors. Results from this study indicated that *C. fistula* might be a beneficial natural resource for treating diarrhea, hyperglycemia, and pain. However, additional

* Corresponding author. Bangladesh Reference Institute for Chemical Measurements (BRiCM), Laboratory Road, Dhaka, 1205, Bangladesh.

** Corresponding author.

E-mail addresses: taher.du.pharma@gmail.com (M.A. Taher), dg.mic@bricm.gov.bd (M. Khan).

<https://doi.org/10.1016/j.heliyon.2024.e28460>

Received 6 November 2023; Received in revised form 17 March 2024; Accepted 19 March 2024

Available online 27 March 2024

2405-8440/© 2024 The Authors. Published by Elsevier Ltd. This is an open access article under the CC BY-NC license (<http://creativecommons.org/licenses/by-nc/4.0/>).

research is required to conduct a comprehensive phytochemical screening and establish precise action mechanisms of the crude extract or the plant-derived compounds.

1. Introduction

Plants represent the most abundant source of many wonderful drugs since the inception of humankind and always offer any type of novel treatments [1–5]. Rigorous laboratory experiments are usually done to justify natural products useful for specific human illnesses [6,7]. Most of the active pharmaceutical ingredients are processed from secondary isolates of plants [8] which have the potential to perform as drugs [9,10] to act against severe conditions [11] which comprises antimicrobial [12,13] and antiviral [14] activity. Conventionally, it is well established that diarrhea and associated problems can be treated through plant or herbal preparations [15]. Due to the various convenient features of herbal drugs, it is widely popular and prescribed by physicians. Therefore, it has become more important to investigate the medicinal compounds [16]. More analgesics have been purified from natural compounds during the past few decades, leading to new structural classes and modes of action [17].

Cassia fistula L. (Caesalpinioideae), alternately labeled as the golden shower, can be found in numerous geographical areas in the world mostly in the Asian, African, and South American regions. The antifungal agent *C. fistula*, which has substantial antifungal action, is also used to treat a variety of diseases [18,19]. This botanical specimen is employed in Ayurvedic medicine for managing diabetes, leucoderma, pruritus, and hematemesis. For erysipelas and skin conditions, the leaf juice is administered [20]. This plant is used to treat skeletal fractures in Sri Lanka [21]. Additionally, several plant parts have been shown to exhibit a variety of pharmacological properties. This plant has demonstrated cytotoxic properties [22], along with the ability to reduce the oxidation process [23]. Another promising capability includes improving liver function [24] which enables lower cholesterol hypocholesterolemic [25]. Moreover, it is reported to perform against bacteria [26], and scholar has reported its ability to functionalize insulin resistance hence lowering the blood glucose level [27].

Previously, it was reported that, Nuclear Magnetic Resonance (^1H and ^{13}C NMR or 2D NMR) was deployed to isolate and elucidate the structure of the plant's compound [28]. Antioxidant properties of the isolated compounds have been established [29]. However, we used a different strategy, using solvent-solvent extraction to extract and isolate bioactive chemicals, which we then analyzed using GC-MS/MS analytical techniques and FTIR to confirm the functional groups. By comparing the isolated compounds' mass spectra with existing literature, their chemical structure and IUPAC nomenclature were ascertained. We searched the molecular base peak as well as the fragmented mass of the targeted compounds by utilizing NIST 2020 software. Taking into account all of these factors, an animal trial was conducted using mice as animal models to assess the antidiarrheal action, an oral glucose tolerance test to assess and reconfirmed the previously reported [30,31] hypoglycemic action. To corroborate the previously evaluated analgesic properties [32], the tail immersion method, in combination with acetic acid-induced writhing activity, was assessed.

Given the significance of structural molecular biology and the pursuit of structure-driven drug discovery, molecular docking has gained popularity in recent years. The tremendous growth in computer usability and processing capabilities and the simplicity of accessing compact chemical and protein libraries have greatly expedited this advancement [33]. Autonomous molecular docking technology typically use a small substrate and a bigger therapeutic target to predict molecular interactions. It accomplishes this by identifying optimal binding orientations and strengths. Although the term "ligand-protein docking" is frequently used, the scope of this process has grown to encompass interactions between proteins. Its uses in drug development are wide-ranging and include virtual screening, lead optimization, mutagenesis study support, and x-ray crystallography guidance [34]. In our study, we have selected five receptors including the kappa opioid receptor, glucose transporter 3 (GLUT 3), cyclooxygenase 2, DHFR, and EGFR to measure the binding affinity of our isolated compounds from GC-MS/MS. Moreover, the ADME/T of the compounds was also evaluated.

2. Material and method

2.1. Plant assembling

Leaves sample of *C. fistula* were picked in January 2022 from Remakri, nearly 50 km from a site in Thanchi Upazila, Bandarban District, in the southeast of Bangladesh. The plant was identified taxonomically and preserved as a voucher specimen number DACB 93484 at the National Herbarium in Mirpur, Dhaka, Bangladesh, for later use.

2.2. GC-MS/MS qualitative investigation

Gas chromatography-mass spectrometry (GC-MS) was used to examine the bioactive chemicals that were extracted from the leaves of *C. fistula* where a well-established method electron impact ionization (EI) method was used having a mass spectrometer named as GC-MS/MS TQ 8040, manufactured by Shimadzu in Japan. A bonded silica capillary column (Rxi-5 ms; 30 m, 0.25 mm ID, and 0.25 μm) was used, and the column temperature was adjusted to 50 °C. By keeping the injection temperature constant at 250 °C, the specimens were introduced using a split-mode injection method. Preheating was performed in the oven. One minute at 500 °C, 2 min at 200 °C, and 7 min at 300 °C were used to preheat the oven. The compound name, structures, and molecular weights of each extract's bioactive ingredients were determined by comparing its mass spectra with the data found in the NIST and Wiley libraries [5,35,36]. It took a total of 39 min to complete the GC-MS run.

2.3. FTIR analysis of plant extracts

The Fourier transform infrared spectrophotometer (FTIR) is an exceptional instrument for recognizing the many types of chemical bonds and functional groups found in substances. The FTIR study was conducted using dried powders of the plant extract. It is recommended to have a humidity-free room to place the FTIR operation. 100 mg of KBr pellet and five mg of the dried extract powder were combined to make the translucent sample disc following a specific procedure. The ground sample from plant specimen was inserted into an FTIR Spectrometer (Shimadzu, IR Affinity1, Japan) with a scanning range of 400–4000 cm^{-1} having a resolution of 4 cm^{-1} .

2.4. Extraction and partitioning process

Following a few days of sun drying, the leaves were cleaned with water. Next, a robust grinding machine at the Phytochemistry Lab at the State University of Bangladesh was used to treat the dried leaves and turn them into a crushed particles. After the leaf was pulverized into a powder, around 3 L of pure methanol (MeOH) was added to a brown reagent vessel (5 L). The container was filled, the cap was put on, and it was kept in storage for 25 days to allow for complete mixing with periodic shaking and stirring. Following this, the entire mixture underwent another filtration step employing Whatman No. 1 filter paper and a fresh cotton plug. Subsequently, the filtrate was evaporated below 40 °C using a vacuum rotary evaporator to yield a gummy mass (approximately 85.5 g). Methanol-enriched fraction underwent fractionation using a technique outlined by Ref. [37] with modifications as described by Ref. [38]. In brief, 90% methanol and 5 g of the crude extract were dissolved in water. The resulting solution was then subjected to fractional separation using solvents of rising polarity, including petroleum ether, chloroform, and ethyl acetate. A low-temperature rotary evaporator was employed for dehumidify all of the non-aqueous fraction in preparation for further analysis. Particularly in our ongoing research, we aimed to work with the methanol (crude) fractions of the plants.

2.5. Experimental animals

In the investigation, Swiss-albino mice were used. Both male and female mice were gathered from the International Centre for Diarrheal Diseases and Research, Bangladesh (ICDDR, B)'s Animal Resource Branch. The mice were aged 4–5 weeks and had weights ranging from 20 to 25 g. The mice were housed in normal polypropylene cages, and the thermal condition and moisture content within the animal facility were maintained at 25 °C and between 60% and 70%, respectively with a 12-h light–dark cycle. All mice were housed in the laboratory setting for a minimum of 3–4 days to allow them to acclimate, considering their high sensitivity to changes in their environment. Standard procedures for handling and using laboratory animals were followed while carrying out the experiments. The State University of Bangladesh's Institutional Ethical Review Committee (SUB-IERC) has examined the ethical concerns critically and given its approval. The study's complete set of protocols and detailed procedures were authorized and approved.

2.6. Determining onset doses for the *in vivo* study

In the *in vivo* model, the test animals received doses of the leaf extract at 200, 400, and 600 mg/kg body weight. One percent Tween 80 in normal saline was added with the precisely weighed samples to create these loading dosages, which were then processed in one way (24 mg on average for 200 mg/kg, 48 mg on average for 400 mg/kg, and 72 mg on average for 600 mg/kg). The suspension's volume was raised to 3.0 mL.

2.7. Design to conduct an *in vivo* study

Five groups of four mice each were put together using the following division of animals. Group I, the control group, received a solution containing 1% Tween 80 in normal saline at a dosage of 10 mL/kg, while Group II, the standard group, was administered standard medication. Groups III, IV, and V received doses of the leaf's methanol extract of 200, 400, and 600 mg/kg, respectively.

2.8. Anti-diarrheal assay

Mice were made ready for the antidiarrheal test by following the castor oil-induced diarrhea method [39,40]. The standard dose of loperamide was given to Group II, while only 1% Tween 80 solutions was provided to the control group. A feeding needle was employed to deliver 0.5 mL of castor oil orally for 30 min to each animal following the administration of the sample and standard doses. Each animal was placed into a separate cage. The floor was adorned with paper towels that could document fecal stains. Over 4 h, the effectiveness of the test samples' ability to prevent diarrhea was observed. Following the delivery of castor oil, data was obtained hourly. Using the following methods, the proportion of defecation inhibition caused by plant extracts was calculated

$$\% \text{ inhibition of defecation} = (M_{\text{control}} - M_{\text{test}}) / M_{\text{control}} \times 100\%$$

where M = average number of occurrences of diarrhea in each group.

2.9. Hypoglycemic assay

In accordance with the methodology described by Peungvicha et al. [41] the oral glucose tolerance test was used to assess the plant extract's (200, 400, and 600 mg/kg) ability to reduce blood sugar levels. Using a feeding needle, sugar syrup was orally administered to five subgroups of animals. After 5 min, each animal in Group I, Group II, Group III, Group IV, and Group V received water, glibenclamide, 24 mg of the trialed extracts, and 48 mg of the trialed extracts and, 72 mg of the trialed extracts respectively. For 3 h, diabetic test strips were used to check blood sugar. The computation provided was utilized to determine the decrease percentage in blood glucose levels:

$$\% \text{ Reduction in blood glucose} = (\text{BG}_{\text{control}} - \text{BG}_{\text{test}}) / \text{BG}_{\text{control}} \times 100\%$$

where BG = mean blood glucose level for individual.

2.10. Central analgesic activity

The central analgesic properties of *C. fistula* extracts were evaluated using the tail immersion experiment, a heat procedure [42]. A solution of morphine in its native state was prepared by diluting the supplied morphine (15 mg/mL) with saline solution, at a dosage of 2 mg/kg administered subcutaneously. A feeding needle was used to orally provide the test substances to the mice. The mouse tail was tested by being submerged in 55 °C hot water. The duration of the dormant phase for each mouse to move its tail after being exposed to warm water was measured at different time intervals (Immediate, half an hour later, an hour later, and an hour and a half later) subsequent to the application of the test samples.

2.11. Peripheral analgesic activity

To evaluate the peripheral analgesic effects of *C. fistula* extracts, a method involving acetic acid-induced writhing was used [43]. The activity of the crude extract was examined using the acetic acid-induced writhing technique. Each subgroup's animals were given a pain inducer called glacial acetic acid. Aspirin and extracts of 24, 48, and 72 mg were given to Groups II, III IV, and V, respectively. After oral administration of the acid, while Tween 80 solution was administered to the control group. Acetic acid is the cause of writhing. Following the intra-peritoneal injection of acetic acid, the number of writhes was tallied over a duration of 10 min. The percentage of writhing inhibition was then computed using the subsequent formula.

$$\% \text{ inhibition of writhing} = (\text{M}_{\text{control}} - \text{M}_{\text{test}}) / \text{M}_{\text{Control}} \times 100\%$$

where M = mean number of abdominal writhing for each group.

2.12. Molecular docking study

An assessment of the binding affinities of specific chemicals found in the methanolic leaves extract of *Cassia Fistula* against several target proteins has been conducted using computer-based strategies. A group of applications including PyRx, PyMoL 2.3, DiscoveryStudio 4.5, and Swiss PDB viewer has been utilized to complete the process.

2.13. Ligand preparation

The 3D SDF structure of identified compounds mentioned in Table was hunted and downloaded from PubChem (<https://pubchem.ncbi.nlm.nih.gov/>) (accessed on 5 July 2023). Additionally, the 3D SDF structures of five standards Lapatinib (PubChem CID_208908), Ciprofloxacin (PubChem CID_2764), Glibenclamide (PubChem CID_3488), Loperamide (PubChem CID_3955), Diclofenac (PubChem CID_3033) were also downloaded from the website [44–46]. The compounds and standards were systematically imported into Discovery Studio 4.5 to generate a ligand library. As a result, the Pm6 semiempirical technique is used to optimize all compounds, which improves the docking precision [47].

2.14. Target protein selection

11 compounds found from the methanol fractions of the extract of *Cassia fistula* leaves were tested by computerized docking to identify their potential activity of cytotoxicity, antimicrobial, hypoglycaemic, anti-diarrheal, and analgesic properties. To evaluate the cytotoxic potential, the 3D crystal structure of the epidermal growth factor receptor (EGFR) [PDB ID: 1XKK] [44] was downloaded from the protein data bank (<https://www.rcsb.org/>) (accessed on 30 June 2023). Similarly, the 3D structure of the dihydrofolate reductase (DHFR) [PDB ID: 4M6J], the glucose transporter 3 (GLUT3) [PDB ID: 4ZWB], the kappa opioid receptor (KOR) [PDB ID: 6VI4], and the cyclooxygenase-2 (COX-2) [PDB ID:1CX2] were downloaded from the site to assess antimicrobial, hypoglycaemic, anti-diarrheal, and analgesic activity respectively [45,46,48].

2.15. Ligand-protein binding

The target molecules' propensities and probable adherence profiles of plant constituents have been estimated using the software-driven ligand-receptor interaction diagram. The highly advanced PyRxAutodock Vina was used to carry out this molecular drug-protein linking approach, and semi-flexible modeling was used for the molecular docking. We have selected the amino acids from the literature and their corresponding IDs. Prior to loading and formatting the protein to the appropriate macromolecule, we verified that the ligands would only bind to that specific biomolecules. During the docking process, amino acids including Leucine 718, Valine 726, Alanine 743, Lysine 745, Methionine 766, Lysine 775, Arginine 776, Leucine 777, Leucine 788, Threonine 790, Glutamine 791, Leucine 792, Methionine 793, Glycine 796, Cysteine 797, Leucine 799, Aspartic acid 800, Arginine 803, Leucine 844, Threonine 854, Aspartic acid 855, and Phenylalanine 856 were specifically targeted for EGFR [44]. Additionally, for the DHFR target, amino acids including Alanine 9, Isoleucine 16, Leucine 93, Serine 92, Arginine 91, Arginine 77, Glutamic acid 78, Serine 76, Leucine 75, Lysine 54, Valine 120, Serine 119, Lysine 55, Threonine 56, Serine 118, and Glycine 117 were designated as the target site. For the protein with PDB code 1R4U, amino acids Arginine 176, Valine 227, Glutamine 228, Asparagine 254, and Histidine 256 were utilized as the target site [45]. Furthermore, for the GLUT3 target, amino acids including Tyrosine 26, Threonine 28, Glycine 29, Valine 30, Leucine 167, Threonine 191, Proline 194, Glutamine 198, Isoleucine 309, Glycine 312, Valine 313, Threonine 347, Tryptophan 410, Leucine 418, and Phenylalanine 442 were chosen for docking [48]. Likewise, for the KOR target, amino acids including Leucine 103, Leucine 107, Serine 136, Isoleucine 137, Tryptophan 140, Isoleucine 180, Tryptophan 183, Leucine 184, Serine 187, Isoleucine 191, Leucine 192, Isoleucine 194, and Valine 195 were designated. Additionally, for the COX2 target, amino acids including Histidine 90, Glutamine 192, Valine 349, Leucine 352, Serine 353, Tyrosine 355, Tyrosine 385, Alanine 516, Phenylalanine 518, Valine 523, Alanine 527, and Serine 530 were selected for docking [46]. The ligands' SD files were imported into PyRxAutoDock Vina's Open Bable tool, and then converted to pdbqt format so that docking against these chosen macromolecules could get the greatest possible match. Additionally, these functional amino sites were contained within a grid box using grid mapping. The center_x = 16.0260721249, center_y = 34.7147556665, center_z = 35.8594863044, and dimension_x = 25.0549472368, dimension_y = 19.5542794449, dimension_z = 32.3462850229 were kept during EGFR docking. For DHFR the grid box was maintained center_x = 3.41895929706, center_y = -3.43057399, center_z = -18.584952838, and dimension_x = 20.9176658577, dimension_y = 27.9165740713, dimension_z = 26.9542148302. While the grid mapping for GLUT3 was fixed to center_x = 111.258876918, center_y = 14.5149866548, center_z = 63.8367662826 and dimension_x = 31.6678938971, dimension_y = 35.8575618898, dimension_z = 26.9656599396. Similarly, the center_x = 54.1586754034, center_y = -50.4638133528, center_z = -16.3133396498, and dimension_x = 14.9316824179, dimension_y = 28.2599958287, dimension_z = 17.9403895121 were fixed as a grid box for kappa opioid receptor (KOR) docking and also the center_x = 23.1905715177, center_y = 21.1248236343, center_z = 15.5994108474 and dimension_x = 21.9363677814, dimension_y = 18.627708761, dimension_z = 25.0537852272 were fixed as a grid box for COX2 docking. At this time, supportive functions were kept as default. After that, a final docking using AutoDock Vina (version 1.1.2) was performed to determine the ligands' affinity for the macromolecule. After that, a final docking using AutoDock Vina (version 1.1.2) was performed to determine the ligands' affinity for the macromolecule. Water molecules and heteroatoms were eliminated from the proteins. The nonpolar hydrogens and Gasteiger charges were retained using preset option during the protein preparation process. All proteins were minimised using UCSF Chimera to reach their lowest energy state. The normal residues were handled with AMBER ff14sB, while additional residues were processed using Gasteiger mode for further analysis [49]. The final step involved conceptualizing the outcome and utilizing BIOVIA Discovery Studio version 4.5 to forecast the best-fitting 2D and 3D models.

2.16. ADME/T analysis

Modern drug design increasingly uses computational methods to evaluate pharmacokinetics (including Absorption, drug-likeness, distribution, metabolism, excretion, and toxicity) and pharmacokinetic assessments. These studies, collectively known as ADMET, are crucial to developing new drugs [2].

One widely utilized approach involves investigating the pharmacological characteristics of compounds, as exemplified by the work conducted at pkcsm (<http://biosig.unimelb.edu.au/pkcsm/prediction>). Moreover, online tools like SwissADME (<http://www.sib.swiss>) have gained prominence for their ability to predict drug likeness, often assessed using the Lipinski rules. Lipinski lays out these guidelines that can indicate whether a substance is orally accessible. To be more precise, for a chemical to be considered orally viable, it must adhere to specific criteria, such as having a molecular weight below 500 amu, fewer than 10 hydrogen bond acceptor sites, and no more than 5 log P values for lipophilicity.

The provided Table 7 displays the outcomes of ADMET analyses and drug-likeness predictions for the compounds under consideration.

2.17. Statistical analysis

Experimental findings from both in vitro and in vivo assays were presented as the mean value accompanied by the standard error of the mean (SEM). Findings were assessed using a paired *t*-test using IBM SPSS Statistics 2023, and statistical significance was characterized by a *p*-value below 0.05. The molecular docking process was conducted thrice, and the average docking scores were presented alongside standard errors, each scoring less than 1% deviation across docking iterations.

3. Result

3.1. Extraction with methanol solvent of *Cassia fistula* and identification of compounds using GC/MS–MS

From Table 1 and Fig. 1, it is found that methanol extract of *Cassia fistula* yields 11 compounds from GC/MS–MS analysis. Various groups of phytochemicals including alkane, alkene, steroid, ester, ketone, and phenol were found in the analysis. To show the relative concentration of each constituent, these compounds are placed with the peak area percentage. Based on the comparative qualitative analysis, the most predominant substance have been determined as 9-Octadecenamide, (Z)- (7.21%), Oxane-4-carboxamide, 2-propyl- (6.63%), 9,12,15-Octadecatrienoic acid, methyl ester, (Z,Z,Z)- (5.68%), Vitamin E (4.89%), Phytol (4.25%), Globulol (1.69%), Neophytadiene (1.49%), Eicosane (1.55%) and beta. Sitosterol (3.16%).

3.2. FTIR data of the extract

In accordance with the values of the peaks in the infrared spectrophotometer (Fig. 2) found in the test material, FTIR spectroscopy was utilized in the current investigation to determine the functional groups. Crude powder material were mixed with KBR to prepare a disc before placed it in IR ray, and the components' characterizing groups were divided according to their peaks. The acquired results demonstrated the existence of the following functional groups in Table 2: alkane, aromatic compounds, alcohol, inter- and intramolecularly bonded –OH group, imine or oxime, ketone or C]C, C₆H₆O group, and R–NH₂ group.

3.3. Anti-diarrheal property

A significant anti-diarrheal effect, which was dose-dependent, was observed in the animal study for both the fractions that were evaluated and the conventional drug loperamide ($p < 0.05$). Castor oil may cause diarrhea in some people for up to 4 h. Its effectiveness was reduced by loperamide 80.0% and by methanol extract of leaf of *C. fistula* at doses 200 mg/kg, 400 mg/kg and 600 mg/kg with the maximum inhibitory effect of 62%, 72% and 70%, respectively (Table 3). All the data showed statistically significant values compared to the control analysis by IBM SPSS paired *t*-test. Test data revealed no significant difference with the standard, confirming the test extract's efficacy as anti-diarrheal activity.

3.4. Hypoglycemic potential

Blood glucose levels were significantly reduced after injection of methanolic soluble fraction (Table 4). The reduction of percent blood glucose depends on dose and time. The maximum hypoglycemic action was demonstrated by the methanol soluble fraction at a dose of 600 mg/kg body weight after 2 h of glucose administration, while glibenclamide, the standard, reduced blood glucose levels by 58.93%.

3.5. Central analgesic activity

Table 5 displays the outcomes of the methanolic extract's central analgesic activity using the tail immersion method. Comparing the tested substances to the reference drug morphine, all of them revealed a significant ($p < 0.05$) slowing of the pain reaction time. At 90 min after loading the plant sample, both the 400 mg/kg and 600 mg/kg methanolic extract significantly increased PRT (Pain Response Time), up to 6.34 ± 0.066 and 7.61 ± 0.189 , respectively, in comparison to the standard morphine (15.64 ± 0.241). In the experimental mice, these extracts demonstrated a possible analgesic effect.

3.6. Peripheral analgesic activity

Table 6 summarizes the findings of the peripheral analgesic activity of the plant extract (200, 400, and 600 mg/kg body weight) in

Table 1
Compounds extracted with Methanol Solvent from *Cassia fistula*.

S.N	Retention Time	Area %	Compound Name	m/z
1	3.74	1.39	3,3-Dimethoxy-2-butanone	89
2	3.795	1.23	1,3-Dioxolane-4-methanol, 2-ethyl-	103
3	14.321	1.49	Neophytadiene	68
4	18.304	5.68	9,12,15-Octadecatrienoic acid, methyl ester, (Z,Z,Z)-	79
5	18.444	4.25	Phytol	71
6	18.588	1.55	Eicosane	57
7	22.607	7.21	9-Octadecenamide, (Z)-	59
8	22.64	6.63	Oxane-4-carboxamide, 2-propyl-	72
9	33.902	4.89	Vitamin E	165
10	37.091	3.16	beta-Sitosterol	73
11	38.927	1.69	Globulol	67

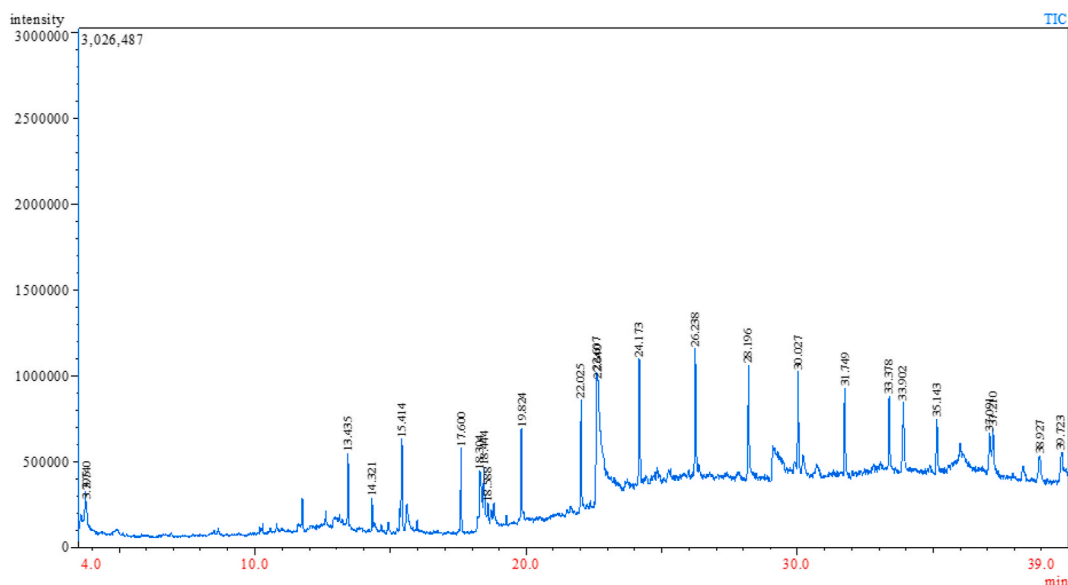


Fig. 1. GC-MS/MS chromatogram of *C. fistula*.

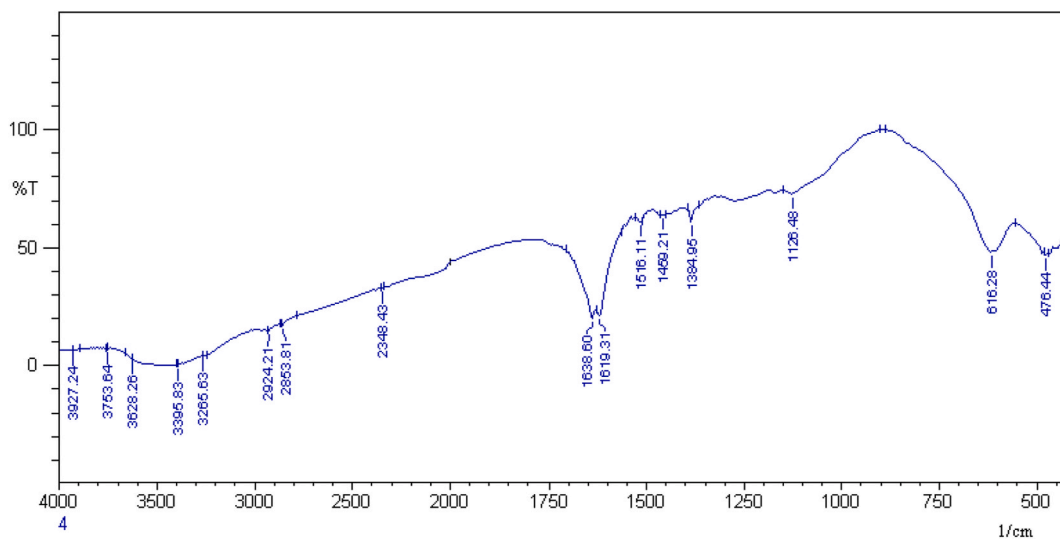


Fig. 2. FTIR chromatogram of methanolic extract.

mice. The use of plant extracts reduced the amount of abdominal writhing that mice experienced after being exposed to acetic acid in a dose-dependent manner, which was statistically significant ($p < 0.05$). This effect was calculated by methanol extract of leaf of *C. fistula* at doses 200 mg/kg, 400 mg/kg and 600 mg/kg with the maximum inhibitory effect of 49.41%, 62% and 56.47%, respectively compared with the standard diclofenac sodium (76.47% inhibition).

3.7. *In silico* investigation (molecular docking)

According to the data presented in Table 7, Compound 10 exhibited the highest binding affinity for the EGFR, scoring -9.4 kcal/mol. Notably, Compounds 9 and 11 also demonstrated a significant affinity for binding to the EGFR, with values of -7.8 and 7.3 kcal/mol, respectively. In comparison, the standard Lapatinib had a binding affinity of -10.6 kcal/mol, indicating its stronger binding capacity. On the other hand, compounds 3, 4, and 5 displayed relatively lower binding affinities of -6.8 kcal/mol against this receptor.

In Fig. 3(a), it can be observed that Compound 10 formed interactions with nine specific amino acids of the EGFR: Leucine 718, Valine 726, Alanine 743, Lysine 745, Methionine 766, Leucine 777, Leucine 788, Cysteine 797, and Leucine 844. Compound 9, conversely, showed bonding with Leucine 718, Valine 726, Alanine 743, Lysine 745, Leucine 792, Methionine 793, Cysteine 797, and

Table 2
FT-IR fingerprint studies and functional groups of the extract of *C. fistula*.

Wavenumber (cm ⁻¹)	Intensity	Functional Group	Compound Class	comments
3927.24, 3753.64		Unknown	Unknown	
3628.26	Moderate, sharp	Hydroxyl stretching	Alcohol	Free
3395.83	High, broad	Hydroxyl stretching	Alcohol	Intermolecular bonded
3265.63	High, broad	Hydroxyl stretching	Carboxylic acid	Usually centered on 3000 cm ⁻¹
2924.21, 2853.81	Low, broad	Hydroxyl stretching	Alcohol	Intra-molecular bonded
	High, broad	Amine stretching	Amine salt	
	Moderate	Sp3 C–H stretching	Alkane	
2348.43	High	O=C=O stretching	Carbon dioxide	
1638.60	Moderate	Ethylene stretching	Alkene	Disubstituted (cis)
	Moderate	N–H bending	Amine	
	Moderate	Pi-bond stretching	Cyclic alkene	
	High	Pi-bond stretching	Alkene	Monosubstituted
1619.31	High	Pi-bond stretching	α,β-Unsaturated ketone	
1516.11	High	N–O stretching	Nitro compound	
1459.21		Unknown		
1384.95	Moderate	O–H bending	Alcohol	
	High	SJO stretching	Sulfate	
	High	SJO stretching	Sulfonyl chloride	
	High	C–F stretching	Fluoro compound	
	Moderate	O–H bending	Phenol	
616.28	High	C–Br stretching	Halo compound	
			Benzene derivative	

Table 3
Effect of methanolic extract of leaf of *C. fistula* L. on castor oil (1mL/mice) induced diarrhea in mice.

Group	Treatment	Number of diarrheal feces (Average ± SEM)	% Reduction of Diarrhea	Significance Vs Control	Significance Vs Std
Group I	Control	12.5 ± 0.29			
Group II	Standard	2.5 ± 0.87**	80	0.003	
Group III	MESF (200 mg/kg)	4.75 ± 0.75**	62	0.002	0.062
Group IV	MESF (400 mg/kg)	3.5 ± 0.65**	72	0.001	0.423
Group V	MESF (600 mg/kg)	3.75 ± 1.18**	70	0.004	0.579

** and * respectively indicate that, the significant p value is less than 0.01 and 0.05 while comparing against control. Number of diarrheal feces represented as Average ± Standard Error of Mean (n = 4), Group I as control group, given 1% Tween 80 in normal saline at a 10 mL/kg body weight dose, Group II (Standard drug loperamide) at 10 mg/kg body weight dose, Group III (MESF 200 = Methanol Soluble Fraction at 200 mg/kg body weight dose); Group IV (MESF 400 = Methanol Soluble Fraction at 400 mg/kg bw dose) and Group V (MESF 600 = Methanol Soluble Fraction at 600 mg/kg body weight dose).

Table 4
The hypoglycemic activity of the methanolic crude extract of the *C. fistula*.

Group	Treatment	BGL 1 H	% Reduction of GL	BGL 2 H	% Reduction of GL	BGL 3H	% Reduction of GL
Group I	Control	11.525 ± 0.295		9.8 ± 0.50		6.325 ± 0.746	
Group II	Standard	7.325 ± 0.3119**	36.41	4.025 ± 0.228	58.93	2.875 ± 0.265*	54.5
Group III	MESF (200 mg/kg)	8.0750 ± 0.2096**	29.90	6.125 ± 0.36**	37.5	4.60 ± 0.212	27.2
Group IV	MESF (400 mg/kg)	8.050 ± 0.4368**	30.12	6.30 ± 0.63*	35.7	4.125 ± 0.165	34.78
Group V	MESF (600 mg/kg)	8.175 ± 0.3145**	29.04	5.45 ± 0.095**	44.39	3.95 ± 0.086*	37.5

**and * respectively indicate that, the significant p value is less than 0.01 and 0.05 while comparing against control; BGL indicated as average ± Standard Error of Mean (n = 4). BGL = Blood glucose level, Group I as control group, given 1% Tween 80 in normal saline at a 10 mL/kg body weight dose, Group II (Standard drug glibenclamide) at 10 mg/kg body weight dose, Group III (MESF 200 = Methanol Soluble Fraction at 200 mg/kg body weight dose); Group IV (MESF 400 = Methanol Soluble Fraction at 400 mg/kg bw dose) and Group V (MESF 600 = Methanol Soluble Fraction at 600 mg/kg body weight dose).

Leucine 844 amino acids. Furthermore, Compound 11 exhibited interactions with Leucine 718, Valine 726, Alanine 743, Lysine 745, Cysteine 797, Leucine 844, and Threonine 854 amino acids. Leucine 718, Serine 720, Valine 726, Alanine 743, Lysine 745, Methionine 766, Leucine 777, Methionine 793, Leucine 844, and Phenylalanine 856 were among the 10 amino acids of the EGFR that the standard Lapatinib showed interaction.

Compound 10 exhibited the highest binding affinity (−8.5 kcal/mol) against DHFR. Notably, Compounds 9 and 11 also demonstrated considerable affinity for DHFR with scores of −6.7 and −6.9 kcal/mol, respectively. In comparison, the standard Ciprofloxacin had a binding affinity of −8.2 kcal/mol (Table 7). Upon examination of Fig. 3(b), it can be observed that Compound 10 interacted with

Table 5
Central analgesic effect of methanolic extract of *C. fistula*.

Group	Treatment	Average time of tail immersion of Mice Time in Sec after Loading the Plant Sample/Drug		
		30 min	60 min	90 min
Group I	Control	2.158 ± 0.0834	2.15 ± 0.03894	2.68 ± 0.10638
Group II	Standard	5.293 ± 0.0825**	10.018 ± 0.2732**	15.64 ± 0.241**
Group III	MESF (200 mg/kg)	2.995 ± 0.0924*	4.268 ± 0.0423**	5.403 ± 0.14505**
Group IV	MESF (400 mg/kg)	3.873 ± 0.0727**	4.938 ± 0.0909**	6.345 ± 0.06614**
Group V	MESF (600 mg/kg)	4.158 ± 0.1725**	5.465 ± 0.31415**	7.61 ± 0.18918**

**and * respectively indicate that, the significant p value is less than 0.01 and 0.05 while comparing against control; data indicated as average ± Standard Error of Mean (n = 4). Group I as control group, given 1% Tween 80 in normal saline at a 10 mL/kg body weight dose, Group II (Standard drug morphine 2 mg/kg), Group III (MESF 200 = Methanol Soluble Fraction at 200 mg/kg body weight dose); Group IV (MESF 400 = Methanol Soluble Fraction at 400 mg/kg bw dose) and Group V (MESF 600 = Methanol Soluble Fraction at 600 mg/kg body weight dose).

Table 6
Peripheral analgesic effect of methanolic extract of *C. fistula*.

Group	Treatment	Average of Writhing	%Inhibition	Significance Vs Control	Significance Vs Standard
Group I	Control	21.25 ± 0.478			
Group II	Standard	5 ± 0.70**	76.47	0	
Group III	MESF (200 mg/kg)	10.75 ± 0.85**	49.41	0.003	0.019
Group IV	MESF (400 mg/kg)	8.5 ± 0.288**	60	0	0.027
Group V	MESF (600 mg/kg)	9.25 ± 0.478**	56.47	0	0.031

**and * respectively indicate that, the significant p value is less than 0.01 and 0.05 while comparing against control; data indicated as average ± Standard Error of Mean (n = 4). Group I as control group, given 1% Tween 80 in normal saline at a 10 mL/kg body weight dose, Group II (Reference Diclofenac sodium 50 mg/kg), Group III (MESF 200 = Methanol Soluble Fraction at 200 mg/kg body weight dose); Group IV (MESF 400 = Methanol Soluble Fraction at 400 mg/kg bw dose) and Group V (MESF 600 = Methanol Soluble Fraction at 600 mg/kg body weight dose).

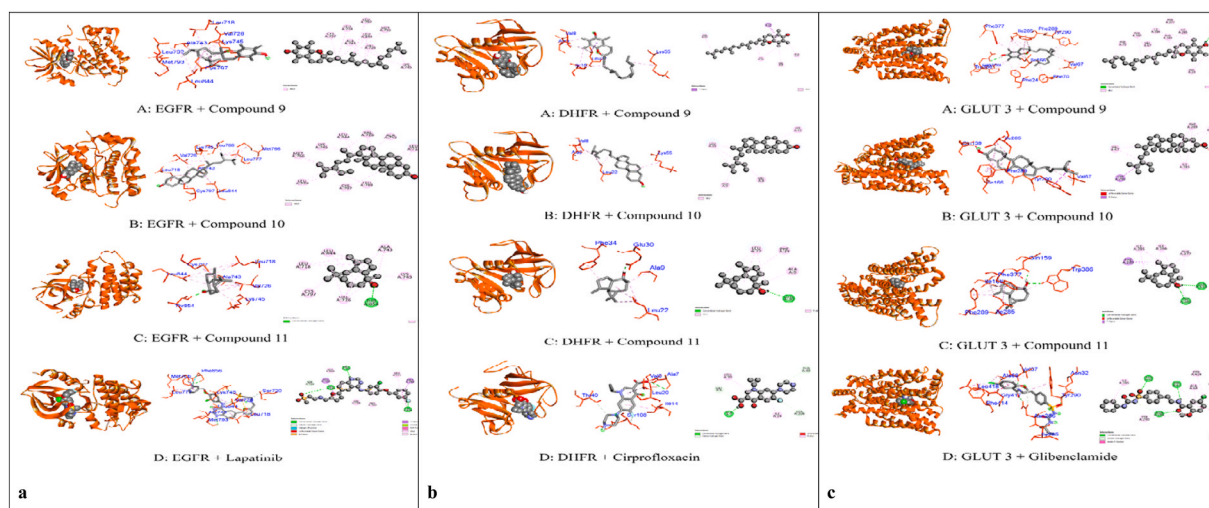


Fig. 3. Graphical depiction illustrating the molecular interactions of the predominant phytocompounds with the (a) EGFR (PDB ID: 1XKK) enzyme with 3D visualization (Compound 9 = A, Compound 10 = B, Compound 11 = C, Standard Lapatinib = D); (b) DHFR (PDB ID: 4M6J) enzyme with 3D visualization (Compound 9 = A, Compound 10 = B, Compound 11 = C, Standard Ciprofloxacin = D.); (c) GLUT 3 (PDB ID: 4ZWB) enzyme with 3D visualization (Compound 9 = A, Compound 10 = B, Compound 11 = C, Standard Glibenclamide = D).

four specific amino acids of DHFR: Valine 8, Alanine 9, Leucine 22, and Lysine 55. Similarly, Fig. 3 (b) revealed that Compound 9 formed interactions with Valine 8, Alanine 9, Isoleucine 16, Leucine 22, and Lysine 55 amino acids. On the other hand, Compound 11 showed interactions with Alanine 9, Leucine 22, Glutamate 30, and Phenylalanine 34 amino acids. In contrast, the standard Ciprofloxacin interacted with Valine 6, Alanine 7, Isoleucine 14, Leucine 20, Threonine 49, and Serine 108 amino acids. Compound 10 demonstrated the highest binding affinity of -9.5 kcal/mol for GLUT3, while Compound 9 also exhibited strong binding affinity with a score of -9.2 kcal/mol. Additionally, Compounds 5 and 11 displayed considerable affinity for binding to GLUT3 with values of -7.1 and 7.9 kcal/mol, respectively. In contrast, the standard Glibenclamide showed a binding affinity of -10.2 kcal/mol. Fig. 3 (c) illustrates that Compound 10 formed interactions with six specific amino acids of GLUT3, including Valine 67, Glutamine 159,

Isoleucine 166, Isoleucine 285, Phenylalanine 289, and Tyrosine 290. Compound 9, the second highest affinity compound, showed interactions with ten amino acids: Phenylalanine 24, Valine 67, Phenylalanine 70, Glutamine 159, Isoleucine 166, Isoleucine 285, Phenylalanine 289, Tyrosine 290, Phenylalanine 377, and Tryptophan 386.

Moreover, Compound 11 was found to interact with six amino acids, namely Glutamine 159, Isoleucine 166, Isoleucine 285, Phenylalanine 289, Phenylalanine 377, and Tryptophan 386. Conversely, the standard Glibenclamide exhibited interactions with nine amino acids of GLUT3, including Asparagine 32, Valine 67, Alanine 68, Isoleucine 285, Asparagine 286, Tyrosine 290, Phenylalanine 414, Glycine 417, and Leucine 418.

For the (KOR), compound 10 showed the highest binding affinity of -9.7 kcal/mol followed by Compound 9 scoring -8.7 kcal/mol. Also, compound 11 showed a strong affinity for binding to the KOR with values of -7.6 kcal/mol. Additionally, compounds 3,4,5 showed -6.8 kcal/mol binding affinities against this receptor, while the standard Loperamide had a binding affinity of -9.1 kcal/mol. Based on Fig. 4(a), Compound 10 exhibited interactions with several amino acids of the kappa opioid receptor, namely Leucine 103, Tyrosine 140, Isoleucine 180, Tryptophan 183, Leucine 184, Isoleucine 191, and Valine 195. Similarly, Compound 9, which had the second-highest affinity, formed bonds with eight different amino acids: Leucine 103, Leucine 107, Tyrosine 140, Isoleucine 180, Tryptophan 183, Leucine 184, Isoleucine 191, and Valine 195. Additionally, Compound 11 showed interactions with the following six amino acids: Leucine 103, Isoleucine 180, Tryptophan 183, Leucine 184, Isoleucine 191, and Serine 192. Loperamide interacted with eight amino acids of the KOR: Isoleucine 96, Phenylalanine 99, Leucine 107, Tyrosine 140, Tryptophan 183, Leucine 184, Isoleucine 191 and Valine 195.

The maximum binding affinity against COX2 was 7.6 kcal/mol, as shown in Table 6, for Compounds 4 and 9. Compounds 3 and 7 exhibited extremely high binding affinities for COX2, scoring -7.3 kcal/mol and 7.3 kcal/mol, respectively. Binding affinities of -7.2 and 6.8 kcal/mol, respectively, were also shown by compounds 5 and 11. In comparison, the common drug Diclofenac had a binding affinity of -7.8 kcal/mol. Analysis of Fig. 4 (b) revealed the specific interactions of each compound with COX2 amino acids. Compound 4 formed bonds with Histidine 90, Valine 116, Valine 349, Leucine 352, Serine 353, Tyrosine 355, Leucine 359, Tyrosine 385, Tryptophan 387, Valine 523, Alanine 527, and Leucine 531.

Compound 9 interacted with Histidine 90, Histidine 95, Valine 349, Leucine 352, Tyrosine 355, Tyrosine 385, Tryptophan 387, Proline 514, Alanine 516, Isoleucine 517, Phenylalanine 518, Valine 523, Glycine 526, Alanine 527, and Leucine 531. Compound 3 was found to interact with Valine 116, Tyrosine 348, Valine 349, Leucine 352, Tyrosine 355, Leucine 359, Tryptophan 387, Phenylalanine 518, Methionine 522, Valine 523, Alanine 527, and Leucine 531. Compound 7 showed interactions with Glutamine 192, Valine 349, Leucine 352, Serine 353, Tyrosine 385, Tryptophan 387, Arginine 513, Phenylalanine 518, Valine 523, Alanine 527, and Leucine 531. Lastly, the standard Diclofenac interacted with Valine 349, Leucine 352, Tyrosine 355, Glycine 526, Alanine 527, and Leucine 531 amino acids.

Broadly speaking, Compounds 9, 10, and 11 exhibited activity across various receptors, except for COX-2, where only Compound 9 displayed significant affinity. However, as depicted in Table 8, none of the compounds adhered to Lipinski's rule of five; each compound had at least one violation. Specifically, Compound 9 displayed three violation indications, implying limited oral bioavailability. In contrast, Compounds 10 and 11 breached two rules, potentially indicating moderate oral bioavailability. Furthermore, the structures of these compounds have been illustrated in Fig. 5.

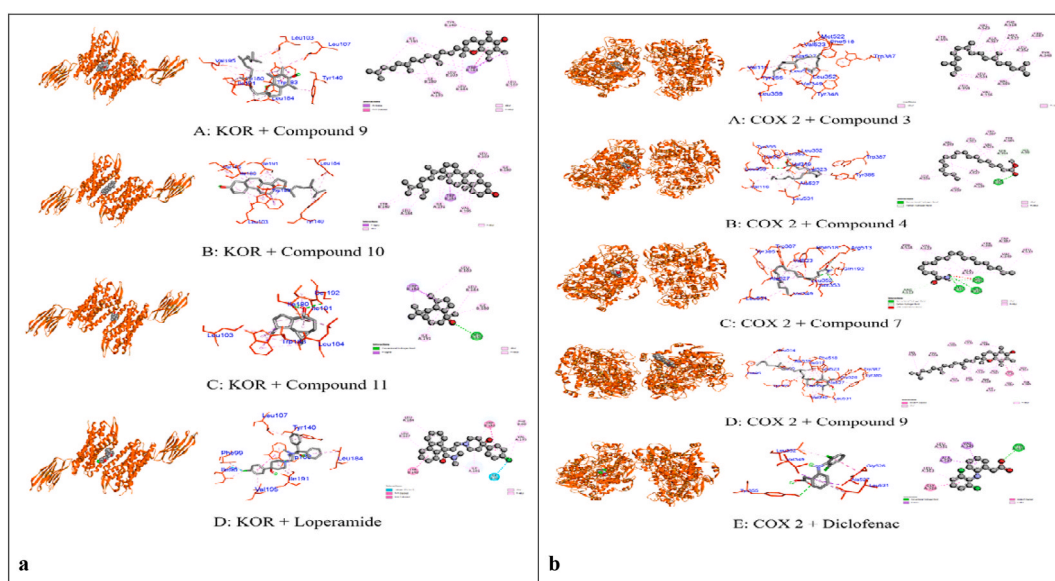


Fig. 4. Graphical depiction illustrating the molecular interactions of the predominant phytocompounds with the (a) KOR (PDB ID: 6VI4) enzyme with 3D visualization (Compound 9 = A, Compound 10 = B, Compound 11 = C, Standard Loperamide = D.); (b) COX 2 (PDB ID: 1CX2) enzyme with 3D visualization (Compound 3 = A, Compound 4 = B, Compound 7 = C, Compound 9 = D, Standard Diclofenac = E).

Table 7
Binding affinities of compounds from methanol fractions of leaves extract of *Cassia fistula* against various receptors.

Binding affinities of compounds from methanol fractions of leaves extract of <i>Cassia fistula</i> against various receptors.								
Methanol	Compound number	Compound Name	Pubchem CID	Binding Affinities				
				EGFR (1XKK)	DHFR (4M6J)	GLUT 3 (4ZWB)	KOR (6VI4)	COX 2 (1CX2)
MEOH	1	3,3-Dimethoxy-2-butanone	140,871	-4.7	-4	-4.8	-3.9	-4.5
MEOH	2	1,3-Dioxolane-4-methanol, 2-ethyl-	546,241	-5.1	-4.6	-5.1	-4.4	-5.1
MEOH	3	Neophytadiene	10,446	-6.8	-5.4	-6.7	-6.8	-7.3
MEOH	4	9,12,15-Octadecatrienoic acid, methyl ester, (Z,Z,Z)-	5,319,706	-6.8	-5.7	-6.6	-6.8	-7.6
MEOH	5	Phytol	5,280,435	-6.8	-5.8	-7.1	-6.8	-7.2
MEOH	6	Eicosane	8222	-5.9	-4.9	-5.9	-6.2	-6.6
MEOH	7	9-Octadecenamide, (Z)-	5,283,387	-6.4	-5.3	-6.6	-6.4	-7.3
MEOH	8	Oxane-4-carboxamide, 2-propyl-	559,220	-6.1	-5.2	-6.2	-5.8	-5.9
MEOH	9	Vitamin E	14,985	-7.8	-6.7	-9.2	-8.7	-7.6
MEOH	10	beta.-Sitosterol	222,284	-9.4	-8.5	-9.5	-9.7	-3
MEOH	11	Globulol	12,304,985	-7.3	-6.9	-7.9	-7.6	-6.8
STD	12	Ciprofloxacin	2764		-8.2			
	13	Lapatinib	208,908	-10.6				
	14	Glibenclamide	3488			-10.2		
	15	Loperamide	3955				-9.1	
	16	Diclofenac	3033					-7.8

hERG channels play a pivotal role in cardiotoxicity, particularly through their involvement in regulating the cardiac action potential. Inhibition of hERG, responsible for the rapid delayed rectifier K⁺ current (I_{Kr}), can lead to prolonged repolarization and QT interval, known as long QT syndrome. This disturbance increases the risk of lethal arrhythmias, such as torsade de pointes, potentially resulting in sudden cardiac death [50]. Table 8 represent no compounds identified from the plant didn't inhibit hERG I representing their safety against cardiotoxicity. Lastly all these compound except Compounds 9 and 10 showed skin sensativity.

4. Discussion

4.1. Prediction and isolation of compounds

GC-MS/MS analysis of the extracts revealed 11 phytochemicals which are displayed in Table 1. Researchers used primary assessment to identify the existence of anthraquinones, flavonoids, saponins, tannins, and terpenoids in the plant *Cassia fistula* [18]. From our GC-MS/MS investigations, in Fig. 6 spectrum A appeared *m/z* value of 68 having mass fragments of 95, 103, and 137 and it has 93% similarity, which was correlated with the parent compound Neophytadiene. According to experts, with the likely involvement of the GABAergic system, diterpenes neophytadiene exerts anxiolytic-like and anticonvulsant effects [6]. Moreover, spectrum B of Fig. 6, having a base peak of 71 showed 95% similarity with the library compound phytol which also showed fragments of 81, 123, and 137. Phytol can augment the level of intracellular reactive oxygen species (ROS) to reduce enzymatic antioxidants such as glutathione peroxidase, which in turn causes DNA damage, which ultimately leads to cell death [51]. Employing the microorganism *Pseudomonas* as a study model, researchers also showed that phytol inhibits the formation of biofilms, reduces ciliary activity, and suppresses the production of pyocyanin [52]. Another compound named Eicosane (Fig. 6, spectrum C) having *m/z* of 57 with 84% similarity has shown fragmentation of 85, 113, 141, 169, and 197. Eicosane, a long-chain hydrocarbon is found to be effective against wound healing properties due to antioxidant capacity, tested by in silico approach [53]. Also (Fig. 6, Spectrum D), manifested *m/z* 165 which correlated with the parent compound vitamin E. Evidence suggests that vitamin E, when administered to leukemia patients, enhances immune activity of dendritic cells (accessory cell) and upregulates the regulation of CD8⁺ proliferation by myeloid-derived suppressor cells (MDSC) [54,55]. Moreover, Beta-sitosterol (Fig. 6, spectrum E) was found to have *m/z* of 73 (fragmentation of 81, 105, and 107) with 76% similarity in the NIST library. It is reported that Beta sitosterol-containing plants show antinociceptive [56], anxiolytic, antibacterial, and antifungal activity having no evidence of perniciousness in brine shrimp cytotoxicity study [57,58]. It has also demonstrated sedative effects [59] in rats, which needs to be evaluated for human also. Additionally, globulol (Fig. 6, spectrum F) is identified with 76% similarity when compared with the NIST library for annotation. Here, the base peak was found to be 67 along with mass fragments of 95, 107, and 135. It is reported that the compound globulol, natural sesquiterpenoids possesses various biological activities, for instance antifungal [60] and antibacterial activities [61].

4.2. In vivo investigations

Medicinal plants have long been employed as remedy to treat a range of digestive issues, particularly diarrhea. Still, not much is known about the reliability and effectiveness of most of the medicinal plants. Consequently, the effectiveness and reliability of *C. fistula* as a possible preventive medication in the treatment of diarrheal sickness were evaluated in this investigation. Diarrhea may result from an imbalance in the smooth muscle action of the gastrointestinal tract or from an abnormality in the absorption pattern of the GI

Table 8
ADME/T studies of identified compounds from leaves of *Cassia fistula*.

S/ N	H- bond Donor	H-bond Acceptors	Lipophilicity - log P (o/w)	GI Absorption	AMES Toxicity	Hepatotoxicity	hERG I inhibitor	Skin Sensitisation	Oral Rat Acute Toxicity (LD50) (mol/kg)	Oral Rat Chronic Toxicity (LOAEL) (log mg/kg bw/ day)	Max. tolerated dose (human) (log mg/kg/ day)	Drug likeliness	Bioavailability score
1	0	3	0.51	High	Yes	No	No	Yes	1.891	2.199	1.107	No; 1 Deviation: MW < 250	0.55
2	1	3	0.53	High	No	No	No	Yes	1.86	2.332	1.122	No; 1 Deviation: MW < 250	0.55
3	0	0	7.07	Low	No	No	No	Yes	1.473	1.158	0.272	No; 2 Deviation: Rotors > 7, XLOGP3 > 3.5	0.55
4	0	2	5.55	High	No	No	No	Yes	1.596	2.932	-0.078	No; 2 Deviation: Rotors > 7, XLOGP3 > 3.5	0.55
5	1	1	6.22	Low	No	No	No	Yes	1.848	1.232	-0.301	No; 2 Deviation: Rotors > 7, XLOGP3 > 3.5	0.55
6	0	0	7.9	Low	No	No	No	Yes	1.586	1.177	-0.014	No; 2 Deviation: Rotors > 7, XLOGP3 > 3.5	0.55
7	1	1	5.32	High	No	No	No	Yes	1.805	0.92	-0.265	No; 2 Deviation: Rotors > 7, XLOGP3 > 3.5	0.55
8	1	2	1.1	High	No	No	No	Yes	1.937	2.589	0.827	No; 1 Deviation: MW < 250	0.55
9	1	2	8.27	Low	No	No	No	No	2.072	1.987	0.775	No; 3 Deviation: MW > 350, Rotors > 7, XLOGP3 > 3.5	0.55
10	1	1	7.19	Low	No	No	No	No	2.552	0.855	-0.621	No; 2 Deviation: MW > 350, XLOGP3 > 3.5	0.55
11	1	1	3.42	High	No	No	No	Yes	1.615	1.187	-0.193	No; 2 Deviation: MW < 250, XLOGP3 > 3.5	0.55

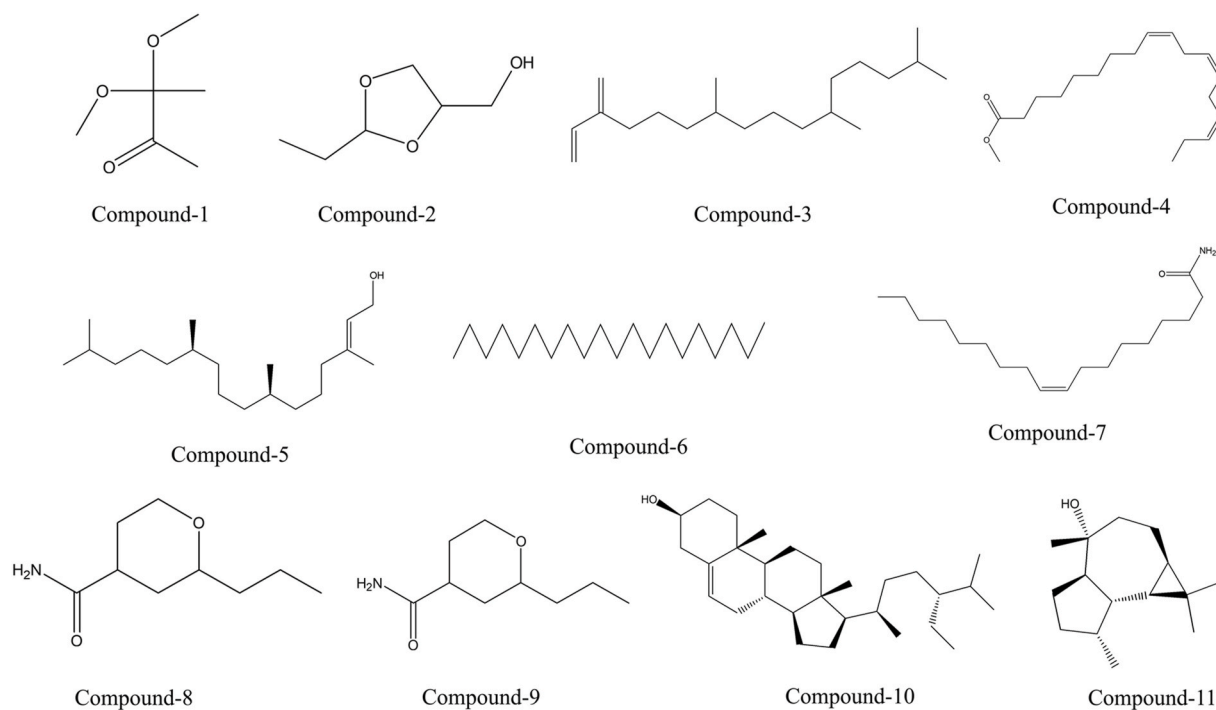


Fig. 5. Structure of the isolated compounds.

tract [62]. It is believed that the main component of castor oil, ricinoleic acid, upsets the gut lining by generating prostaglandins, which might result in diarrhea and peristaltic motion [63,64]. In the animal investigation, crude fractions and the reference drug loperamide showed a substantial ($p < 0.05$) and dose-dependent anti-diarrheal effect. It is reported that beta-sitosterol, found in GC-MS/MS analysis, can act as an anti-diarrheal compound [65] which has been corroborated in the Insilco investigation with kappa receptor. Scientists had reported that, when tocopherol was administered intramuscularly to patients suffering from Shigella dysentery, clinical symptoms decreased and their immunological response improved as compared to those who did not receive tocopherol [66].

To investigate the hypoglycemic activity of this plant, extracts were given to the mice model. After 2 h of glucose delivery, the crude fraction at a dose of 600 mg/kg body mass showed the greatest hypoglycemic activity. Research has demonstrated that by stimulating IR and GLUT4, beta-sitosterol enhances glycemic control in the adipose tissue of rats with type-2 diabetes caused by high fat and sugar [67]. Identified compound globulin has been reported to have antidiabetic properties [68]. Vitamin E has also demonstrated the capability of reducing blood sugar levels in combination with ascorbic acid [69].

The tail immersion method and the mice writhing method were employed in this investigation to evaluate the analgesic effects of methanol extract. In our trial, the mice suffering from acetic acid and heat were much reduced by the plant samples. In assays involving hot plates and acetic acid, isolated β -sitosterol was found to exhibit pain-relieving properties by preventing the synthesis of prostaglandins and bradykinins, suppressing opioid receptors, or encouraging the release of endogenous opioid peptides, as reported by scholars [70]. Phytol, a diterpene has been recorded as an antinociceptive compound experimentally in animal models [71].

4.3. *In silico* investigations

The functions of cells, such as proliferation and apoptosis, are under the control of the Epidermal Growth Factor Receptor (EGFR). When a ligand, like EGF, binds to EGFR, it triggers structural modifications that lead to the phosphorylation of tyrosine residues in the C-terminal segment. This phosphorylation sets off cascades of events, including the activation of signaling pathways like MAPK, PI3K/AKT, and STAT3/STAT5. These pathways act to inhibit cell death (apoptosis) and encourage activities associated with cancer, thereby promoting cancer-related processes [72]. Displaying a substantial potential for binding of -9.4 kcal/mol, Compound 10 engages with EGFR via ten alkyl bonds, while Compound 9 forms bonds with nine alkyl groups, leading to a binding value of -7.8 kcal/mol. Conversely, the reference Lapatinib demonstrates a distinct array of ten bonds against EGFR encompassing hydrogen bond, pi bond, unfavorable donor-donor bond, and others, yielding a binding interaction value of -10.6 kcal/mol (Table 7).

Dihydrofolate reductase (DHFR) holds significant importance as an enzyme within the folate pathway, facilitating the transformation of dihydrofolic acid (DHF) into tetrahydrofolic acid (THF). THF plays a crucial role in synthesizing the building blocks (amino acids) and genetic material, vital components for the growth and multiplication of cells. Disruption of the folate pathway causes unregulated cell proliferation, ultimately contributing to the development of diverse cancer types [73]. Interacting with DHFR,

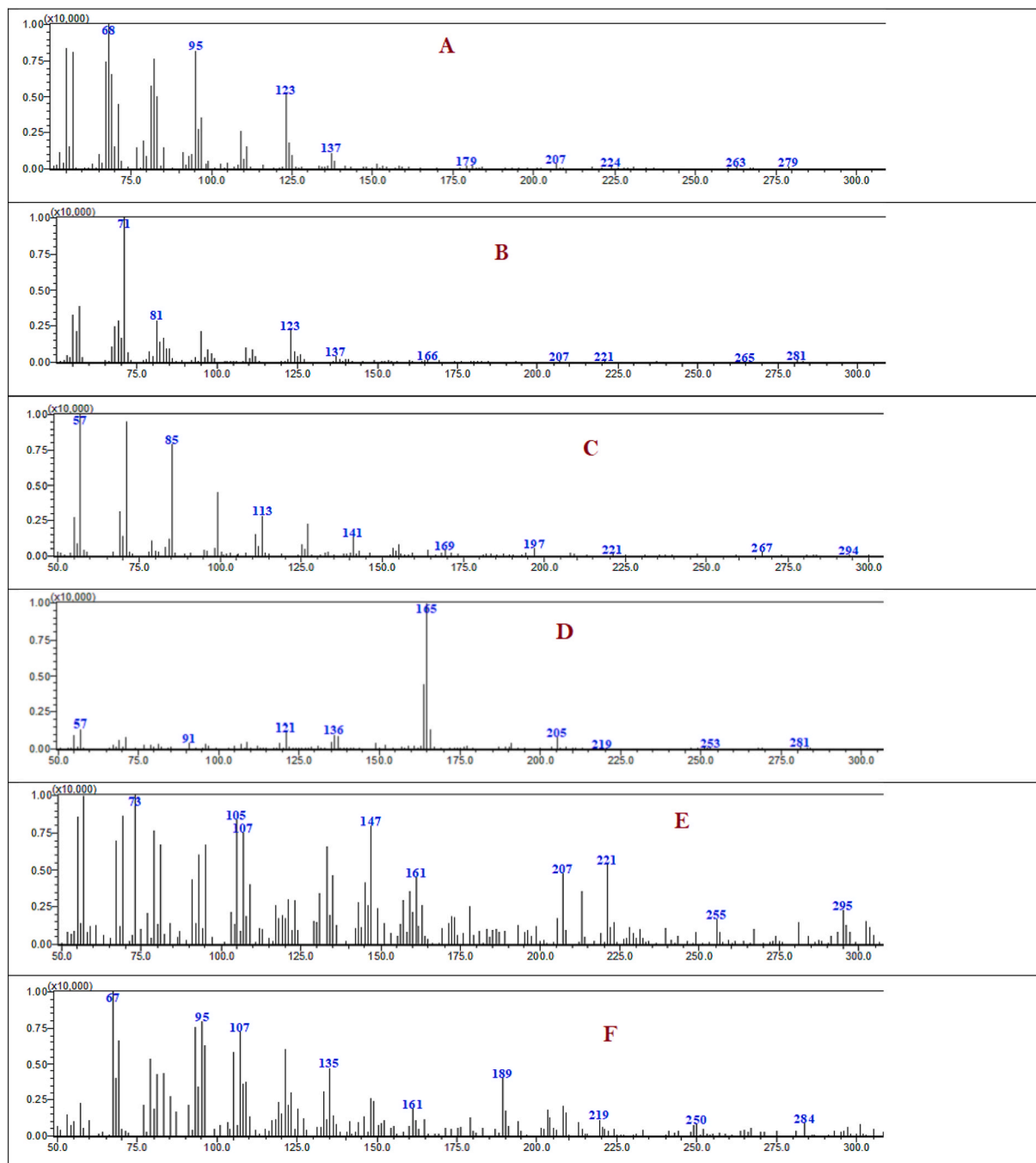


Fig. 6. Relative Intensity vs. m/z spectrum of compounds Neophytadiene (Spectrum A), Phytol (Spectrum B), Eicosane (Spectrum C), Vitamin E (Spectrum D), Beta-sitosterol (Spectrum E), Globulol (Spectrum F).

Compound 10 establishes four alkyl bonds, showcasing a substantial affinity of -8.5 kcal/mol, surpassing the reference binding value of -8.2 kcal/mol held by Ciprofloxacin. In contrast, Ciprofloxacin attaches via one conventional hydrogen bond, an unfavorable donor-donor bond, an alkyl bond, and three carbon-hydrogen bonds, while Compound 11 binds with one conventional hydrogen bond and three alkyl bonds, yielding a binding score of -6.9 kcal/mol (Table 7).

The glucose transporter protein called GLUT3 enables the concentration-dependent passive transport of glucose across cell membranes. By enabling glucose to enter or exit cells based on glucose concentrations, it helps to manage blood glucose levels. This is especially true of the liver, kidney, and pancreatic cells [74]. In Fig. 3 (c) it is depicted that Compound 10 engaged with the GLUT-3 receptor via an unfavorable donor-donor bond, one pi-sigma interaction, and four pi-alkyl bonds, yielding a noteworthy binding

affinity of -9.5 kcal/mol. On the other hand, Compound 9 exhibited interaction through a conventional hydrogen bond, along with five pi-alkyl bonds and four alkyl bonds, displaying an affinity of -9.2 kcal/mol when compared to Glibenclamide's -10.2 kcal/mol.

The μ , κ , and δ opioid receptors found in the human GI tract regulate GI signaling by reducing the activity of enteric nerves, lowering the release of neurotransmitters, and blocking pathways that are both excitatory and inhibitory. This causes changes in stool consistency and motility, a slowing of colonic transit, a decrease in the excitability of enteric neurons, and alterations to secretion and fluid transport [75]. Demonstrating potent binding affinity to the κ -opioid receptor, Compound 10 surpasses the standard value of Loperamide, forming a complex with the receptor through the engagement of five alkyl bonds and a solitary pi-sigma interaction. However, Compound 9 also conveyed potential affinity towards the receptor with six alkyl and pi-sigma bonds.

Prostaglandins, especially PGE2, are produced due to elevated COX-2 expression, which is triggered by factors such as substances that cause inflammation. These substances are essential for both producing and controlling inflammatory pain. Inhibiting COX-2 is essential for reducing inflammation-related discomfort and hypersensitivity [76]. Compounds 4 and 9 displayed a remarkable affinity for COX-2 receptors, binding at -7.6 kcal/mol, slightly below Diclofenac's -7.8 kcal/mol (Table 6). This interaction led to various bonds in compound 4, including a conventional hydrogen bond, two carbon-hydrogen bonds, five alkyl bonds, and three pi-alkyl bonds. Similarly, compound 9 exhibited one amide-pi bond, nine alkyl bonds, and five pi-alkyl bonds, illustrating the attraction against COX-2 in Fig. 4 (b).

However, there are some limitations of the ADME/T study. pkCSM and SwissADME are limited by the quality of their experimental data, which may result in mistakes when dealing with incomplete datasets. These technologies, which use simplified models, can have difficulty predicting unexpected chemical reactions and may not account for species-specific differences or dynamic changes in biological systems. The specified criteria for physicochemical parameters are generalizations, and discrepancies may occur among multiple computational tools. As a result, further expanded ADME/T analysis, especially in a clinical setting, is recommended to establish those compounds' drug-like candidacy.

5. Conclusion

Phytochemical studies of the plant *C. fistula* through Gas Chromatography provides important phytochemicals which undergoes in silico analysis. Among 11 compounds, Vitamin E, Beta-Sitosterol and Globulol found effective in molecular binding against various receptors including EGFR, DHFR, GLUT 3 and KOR .9,12,15-Octadecatrienoic acid, methyl ester, (Z,Z,Z), 9-Octadecenamamide, (Z), Vitamin E and Neophytadiene provides good binding affinity towards COX2 receptor. This molecular investigation corroborates with the in vivo findings of the plant extract which might offer an entirely new viewpoint on controlling diarrhea, hyperglycemia, pain as well as cytotoxicity and infections. However, there is a need for further study to investigate the mechanism of action.

Ethical approval

The biological activity assays were carried out in accordance with the 2013 Helsinki Declaration's ethical guidelines. The Swiss Academy of Medical Sciences' guiding standards were followed when handling and caring for animal models.

Ethical Committee Name: Institutional Ethical Review Committee (SUB-IERC), State University of Bangladesh.

Approval Number: 2023-01-04/SUB/A-ERC/001.

Funding

This research was not supported by a specific grant from any governmental, private, or nonprofit funding sources.

Data availability statement

Data will be made available on request.

CRediT authorship contribution statement

Mohammad Abdullah Taher: Writing – review & editing, Writing – original draft, Validation, Software, Methodology, Investigation, Formal analysis, Data curation, Conceptualization. **Aysha Akter Laboni:** Conceptualization. **Md Ashrafur Islam:** Resources. **Hasin Hasnat:** Software. **Mohammad Mahmudul Hasan:** Writing – review & editing. **Jannatul Ferdous:** Software. **Suriya Akter Shompa:** Formal analysis. **Mala Khan:** Validation, Supervision, Resources, Project administration, Conceptualization.

Declaration of competing interest

The authors declare that they have no known competing financial interests or personal relationships that could have appeared to influence the work reported in this paper

Appendix A. Supplementary data

Supplementary data to this article can be found online at <https://doi.org/10.1016/j.heliyon.2024.e28460>.

References

- [1] M.M. Hasan, M.S. Hossain, M.A. Taher, T. Rahman, Evaluation of analgesic, anti-diarrheal and hypoglycemic activities of *Wendlandia paniculata* (Roxb.) DC leaves extract using mice model, *Toxicol. Int.* 28 (2021) 155–163.
- [2] M.M. Hasan, M.A. Taher, M.A. Rahman, T. Muslim, Analgesic, anti-diarrheal, CNS-depressant, membrane stabilizing and cytotoxic activities of *Canavalia virosa* (Roxb.) W&A, *Banglades. Pharm. J.* 22 (2019) 214–218.
- [3] A.A.H. Pinkey, Z.I. Khan, M.A. Taher, M.A. Soma, *Elaeocarpus serratus* L. Exhibits potential analgesic and anti-diarrheal activities in mice model, *Int. J. 6* (2020) 44–51.
- [4] A. Rahman, M.M. Hasan, M.A. Taher, T. Muslim, Analgesic, anti-diarrheal and CNS-depressant activities of *Flemingia macrophylla* (Willd.), *Banglades. Pharm. J.* 23 (2020) 141–145.
- [5] M.A. Taher, A.A. Laboni, S.A. Shompa, M.M. Rahman, M.M. Hasan, H. Hasnat, M. Khan, Bioactive compounds extracted from leaves of *G. Cyanocarpa* using various solvents in chromatographic separation showed anti-cancer and anti-microbial potentiality in in silico approach, *Chin. J. Anal. Chem.* (2023) 100336, <https://doi.org/10.1016/j.cjac.2023.100336>.
- [6] M.L. Gonzalez-Rivera, J.C. Barragan-Galvez, D. Gasca-Martínez, S. Hidalgo-Figueroa, M. Isirdia-Espinoza, A.J. Alonso-Castro, In vivo neuropharmacological effects of neophytadiene, *Molecules* 28 (2023) 3457.
- [7] B.-J. Guo, Z.-X. Bian, H.-C. Qiu, Y.-T. Wang, Y. Wang, Biological and clinical implications of herbal medicine and natural products for the treatment of inflammatory bowel disease, *Ann. N. Y. Acad. Sci.* 1401 (2017) 37–48.
- [8] F. Bourgaud, A. Gravot, S. Milesi, E. Gontier, Production of plant secondary metabolites: a historical perspective, *Plant Sci.* 161 (2001) 839–851.
- [9] H.I.A. Boy, A.J.H. Rutilla, K.A. Santos, A.M.T. Ty, I.Y. Alicia, T. Mahboob, J. Tangpoong, V. Nissapatorn, Recommended medicinal plants as source of natural products: a review, *Digit. Chin. Med.* 1 (2018) 131–142.
- [10] S.M. Mawalagedera, D.L. Callahan, A.C. Gaskett, N. Rønsted, M.R. Symonds, Combining evolutionary inference and metabolomics to identify plants with medicinal potential, *Front. Ecol. Evol.* 7 (2019) 267.
- [11] M.G. Moloney, Natural products as a source for novel antibiotics, *Trends Pharmacol. Sci.* 37 (2016) 689–701.
- [12] U. Anand, N. Jacobo-Herrera, A. Altemimi, N. Lakhssassi, A comprehensive review on medicinal plants as antimicrobial therapeutics: potential avenues of biocompatible drug discovery, *Metabolites* 9 (2019) 258.
- [13] K. Bazaka, M.V. Jacob, W. Chrzanowski, K. Ostrikov, Anti-bacterial surfaces: natural agents, mechanisms of action, and plasma surface modification, *RSC Adv.* 5 (2015) 48739–48759.
- [14] P. Gupta, P. Bhattar, D. D'souza, M. Tolani, P. Daswani, P. Tetali, T. Birdi, Evaluating the anti *Mycobacterium tuberculosis* activity of *Alpinia galanga* (L.) Willd. axenically under reducing oxygen conditions and in intracellular assays, *BMC Compl. Alternative Med.* 14 (2014) 1–8.
- [15] P. Rawat, P.K. Singh, V. Kumar, Evidence based traditional anti-diarrheal medicinal plants and their phytochemicals, *Biomed. Pharmacother.* 96 (2017) 1453–1464, <https://doi.org/10.1016/j.biopha.2017.11.147>.
- [16] P.K. Mukherjee, K. Maiti, K. Mukherjee, P.J. Houghton, Leads from Indian medicinal plants with hypoglycemic potentials, *J. Ethnopharmacol.* 106 (2006) 1–28, <https://doi.org/10.1016/j.jep.2006.03.021>.
- [17] C.R. McCurdy, S.S. Scully, Analgesic substances derived from natural products (natureceuticals), *Life Sci.* 78 (2005) 476–484, <https://doi.org/10.1016/j.lfs.2005.09.006>.
- [18] S.L. Jothy, Z. Zakaria, Y. Chen, Y.L. Lau, L.Y. Latha, S. Sasidharan, Acute oral toxicity of methanolic seed extract of *Cassia fistula* in mice, *Molecules* 16 (2011) 5268–5282.
- [19] V.P. Kumar, N.S. Chauhan, H. Padh, M. Rajani, Search for antibacterial and antifungal agents from selected Indian medicinal plants, *J. Ethnopharmacol.* 107 (2006) 182–188.
- [20] R.N. Chopra, S.L. Nayar, Glossary of Indian Medicinal Plants, Council of Scientific and Industrial Research, 1956.
- [21] D.T. Ekanayake, Plants used in the treatment of skeletal fractures in the indigenous system of medicine in Sri Lanka, *Sri Lanka For.* 14 (1980) 145–152.
- [22] M. Gupta, U.K. Mazumder, N. Rath, D.K. Mukhopadhyay, Antitumor activity of methanolic extract of *Cassia fistula* L. seed against Ehrlich ascites carcinoma, *J. Ethnopharmacol.* 72 (2000) 151–156.
- [23] A. Luximon-Ramma, T. Bahorun, M.A. Soobrattee, O.I. Aruoma, Antioxidant activities of phenolic, proanthocyanidin, and flavonoid components in extracts of *Cassia fistula*, *J. Agric. Food Chem.* 50 (2002) 5042–5047.
- [24] T. Bhakta, P.K. Mukherjee, K. Mukherjee, S. Banerjee, S.C. Mandal, T.K. Maity, M. Pal, B.P. Saha, Evaluation of hepatoprotective activity of *Cassia fistula* leaf extract, *J. Ethnopharmacol.* 66 (1999) 277–282.
- [25] S.S. El-Saadany, R.A. El-Massry, S.M. Labib, M.Z. Sitohy, The biochemical role and hypocholesterolaemic potential of the legume *Cassia fistula* in hypercholesterolaemic rats, *Food Nahrung* 35 (1991) 807–815.
- [26] R.P. Samy, S. Ignacimuthu, A. Sen, Screening of 34 Indian medicinal plants for antibacterial properties, *J. Ethnopharmacol.* 62 (1998) 173–181.
- [27] A. Díaz, I. de Gracia, R. de Tello, M.P. Gupta, Evaluation of traditional medicine: effects of *Cajanus cajan* L. and of *Cassia fistula* L. on carbohydrate metabolism in mice, *Rev. Med. Panama* 16 (1991) 39–45.
- [28] L.M. da Silva, L.F.S. Araújo, R.C. Alvez, L. Ono, D.A.T. Sá, P.L.R. da Cunha, R.C. Monteiro de Paula, J.S. Maciel, Promising alternative gum: extraction, characterization, and oxidation of the galactomannan of *Cassia fistula*, *Int. J. Biol. Macromol.* 165 (2020) 436–444, <https://doi.org/10.1016/j.jbiomac.2020.09.164>.
- [29] A. Goldson Barnaby, R. Reid, V. Rattray, R. Williams, M. Denny, Characterization of Jamaican *Delonix regia* and *Cassia fistula* seed extracts, *Biochem. Res. Int.* 2016 (2016) e3850102, <https://doi.org/10.1155/2016/3850102>.
- [30] M.M. Rahman, M.J. Uddin, A.S.M.A. Reza, A.M. Tareq, T.B. Emran, J. Simal-Gandara, Ethnomedicinal value of antidiabetic plants in Bangladesh: a comprehensive review, *Plants* 10 (2021) 729, <https://doi.org/10.3390/plants10040729>.
- [31] B. Salehi, A. Ata, N.V. Anil Kumar, F. Sharopov, K. Ramírez-Alarcón, A. Ruiz-Ortega, S. Abdulmajid Ayatollahi, P. Valere Tsouh Fokou, F. Kobarfard, Z. Amiruddin Zakaria, M. Iriti, Y. Taheri, M. Martorell, A. Sureda, W.N. Setzer, A. Durazzo, M. Lucarini, A. Santini, R. Capasso, E. Adrian Ostrander, A. ur-Rahman, M. Iqbal Choudhary, W.C. Cho, J. Sharifi-Rad, Antidiabetic potential of medicinal plants and their active components, *Biomolecules* 9 (2019) 551, <https://doi.org/10.3390/biom9100551>.
- [32] P. Antonisamy, P. Agastian, C.-W. Kang, N.S. Kim, J.-H. Kim, Anti-inflammatory activity of rhein isolated from the flowers of *Cassia fistula* L. and possible underlying mechanisms, *Saudi J. Biol. Sci.* 26 (2019) 96–104, <https://doi.org/10.1016/j.sjbs.2017.04.011>.
- [33] G.M. Morris, M. Lim-Wilby, Molecular modeling of proteins, *Methods Mol. Biol.* 443 (2008) 365–382.
- [34] A. Pozzan, Molecular descriptors and methods for ligand based virtual high throughput screening in drug discovery, *Curr. Pharmaceut. Des.* 12 (2006) 2099–2110.
- [35] S. Kim, P.A. Thiessen, E.E. Bolton, J. Chen, G. Fu, A. Gindulyte, L. Han, J. He, S. He, B.A. Shoemaker, PubChem substance and compound databases, *Nucleic Acids Res.* 44 (2016) D1202–D1213.
- [36] A.J. Obaidullah, M.M. Alanazi, N.A. Alsaif, W.A. Mahdi, O.I. Fantoukh, A.M. Tareq, S.A. Sami, A.M. Alqahtani, T.B. Emran, Deeper insights on cnesmone javanica blume leaves extract: chemical profiles, biological attributes, network pharmacology and molecular docking, *Plants* 10 (2021) 728.
- [37] S.M. Kupchan, G. Tsou, Tumor Inhibitors. LXXXI. Structure and partial synthesis of fabacein, *J. Org. Chem.* 38 (1973) 1055–1056.
- [38] B.C. VanWagenen, R. Larsen, J.H. Cardellina, D. Randazzo, Z.C. Lidert, C. Swithenbank, Ulosantoin, a potent insecticide from the sponge *Ulosa ruetzleri*, *J. Org. Chem.* 58 (1993) 335–337.
- [39] F.G. Shoba, M. Thomas, Study of anti-diarrhoeal activity of four medicinal plants in castor-oil induced diarrhoea, *J. Ethnopharmacol.* 76 (2001) 73–76.
- [40] M. Sisay, E. Engidawork, W. Shibeshi, Evaluation of the anti-diarrheal activity of the leaf extracts of *Myrtus communis* Linn (Myrtaceae) in mice model, *BMC Compl. Alternative Med.* 17 (2017) 1–11.

- [41] P. Peungvicha, S.S. Thirawarapan, R. Temsiririrkkul, H. Watanabe, J.K. Prasain, S. Kadota, Hypoglycemic effect of the water extract of *Piper sarmentosum* in rats, *J. Ethnopharmacol.* 60 (1998) 27–32.
- [42] M.I. Ezeja, Y.S. Omeh, I.I. Ezeigbo, A. Ekechukwu, Evaluation of the analgesic activity of the methanolic stem bark extract of *Dialium guineense* (Wild), *Ann. Med. Health Sci. Res.* 1 (2011) 55–62.
- [43] R. Koster, Acetic acid for analgesics screening, *Fed Proc.* (1959) 412–417.
- [44] I.H. El Azab, H.S. El-Sheshatowy, R.B. Bakr, N.A. Elkanzi, New 1, 2, 3-triazole-containing hybrids as antitumor candidates: design, click reaction synthesis, DFT calculations, and molecular docking study, *Molecules* 26 (2021) 708.
- [45] M.C.S. Khatun, M.A. Muhi, M.J. Hossain, M.A. Al-Mansur, S.A. Rahman, Isolation of phytochemical constituents from *Stevia rebaudiana* (Bert.) and evaluation of their anticancer, antimicrobial and antioxidant properties via *in vitro* and *in silico* approaches, *Heliyon* 7 (2021) 1.
- [46] N. Muhammad, R. Lal Shrestha, A. Adhikari, A. Wadood, H. Khan, A.Z. Khan, F. Maione, N. Mascolo, V. De Feo, First evidence of the analgesic activity of govaniadine, an alkaloid isolated from *Corydalis govaniana* Wall, *Nat. Prod. Res.* 29 (2015) 430–437.
- [47] S. Mahmud, M.O. Rafi, G.K. Paul, M.M. Promi, M.S.S. Shimu, S. Biswas, T.B. Emran, K. Dhama, S.A. Alyami, M.A. Moni, Designing a multi-epitope vaccine candidate to combat MERS-CoV by employing an immunoinformatics approach, *Sci. Rep.* 11 (2021) 15431.
- [48] L. Mojica, E.G. de Mejia, M.A. Granados-Silvestre, M. Menjivar, Evaluation of the hypoglycemic potential of a black bean hydrolyzed protein isolate and its pure peptides using *in silico*, *in vitro* and *in vivo* approaches, *J. Funct. Foods* 31 (2017) 274–286.
- [49] M.V. Shapovalov, R.L. Dunbrack, A smoothed backbone-dependent rotamer library for proteins derived from adaptive kernel density estimates and regressions, *Structure* 19 (2011) 844–858, <https://doi.org/10.1016/j.str.2011.03.019>.
- [50] S. Kalyanamoorthy, K.H. Barakat, Development of safe drugs: the hERG challenge, *Med. Res. Rev.* 38 (2018) 525–555, <https://doi.org/10.1002/med.21445>.
- [51] A. Bouyahya, I. Chamkhi, A. Balahbib, M. Rebezov, M.A. Shariati, P. Wilairatana, M.S. Mubarak, T. Benali, N. El Omari, Mechanisms, anti-quorum-sensing actions, and clinical trials of medicinal plant bioactive compounds against bacteria: a comprehensive review, *Molecules* 27 (2022) 1484.
- [52] B. Pejin, A. Ciric, J. Glamoclija, M. Nikolic, M. Sokovic, *In vitro* anti-quorum sensing activity of phytol, *Nat. Prod. Res.* 29 (2015) 374–377.
- [53] A. Balachandran, S.B. Choi, M.-M. Beata, J. Małgorzata, G.R. Froemming, C.A. Lavilla Jr., M.P. Billacura, S.N. Siyumbwa, P.N. Okechukwu, Antioxidant, wound healing potential and *in silico* assessment of Naringin, Eicosane and Octacosane, *Molecules* 28 (2023) 1043.
- [54] T.H. Kang, J. Knoff, W.-H. Yeh, B. Yang, C. Wang, Y.S. Kim, T.-C. Wu, C.-F. Hung, Treatment of tumors with vitamin E suppresses myeloid derived suppressor cells and enhances CD8⁺ T cell-mediated antitumor effects, *PLoS One* 9 (2014) e103562.
- [55] X. Yuan, Y. Duan, Y. Xiao, K. Sun, Y. Qi, Y. Zhang, Z. Ahmed, D. Moiani, J. Yao, H. Li, Vitamin E enhances cancer immunotherapy by reinvigorating dendritic cells via targeting checkpoint SHP1, *Cancer Discov.* 12 (2022) 1742–1759.
- [56] M.S. Bin Sayeed, S.M.R. Karim, T. Sharmin, M.M. Morshed, Critical analysis on characterization, systemic effect, and therapeutic potential of beta-sitosterol: a plant-derived orphan phytosterol, *Medicines* 3 (2016) 29.
- [57] P.C. Kiprono, F. Kaberia, J.M. Keriko, J.N. Karanja, The *in vitro* anti-fungal and anti-bacterial activities of β -sitosterol from *Senecio lyratus* (Asteraceae), *Z. Naturforsch. C Biosci.* 55 (2000) 485–488.
- [58] G. Mishra, P. Singh, R. Verma, S. Kumar, S. Srivastav, K.K. Jha, R.L. Khosa, Traditional uses, phytochemistry and pharmacological properties of *Moringa oleifera* (an overview), *Der Pharm. Lett.* 3 (2011) 141–164.
- [59] C. López-Rubalcava, B. Piña-Medina, R. Estrada-Reyes, G. Heinze, M. Martínez-Vázquez, Anxiolytic-like actions of the hexane extract from leaves of *Annona cherimolia* in two anxiety paradigms: possible involvement of the GABA/benzodiazepine receptor complex, *Life Sci.* 78 (2006) 730–737.
- [60] M. Tan, L. Zhou, Y. Huang, Y. Wang, X. Hao, J. Wang, Antimicrobial activity of globulol isolated from the fruits of *Eucalyptus globulus* Labill, *Nat. Prod. Res.* 22 (2008) 569–575.
- [61] M.S.M. Luna, R.A. De Paula, R.B. Costa, J.V. Dos Anjos, M.V. Da Silva, M.T.S. Correia, Bioprospection of *Libidibia ferrea* var. *ferrea*: phytochemical properties and antibacterial activity, *South Afr. J. Bot.* 130 (2020) 103–108.
- [62] J. Gidudu, D.A. Sack, M. Pina, M.J. Hudson, K.S. Kohl, P. Bishop, A. Chatterjee, E. Chiappini, A. Compingbutra, C. Da Costa, Diarrhea: case definition and guidelines for collection, analysis, and presentation of immunization safety data, *Vaccine* 29 (2011) 1053. https://www.researchgate.net/profile/Jane-Gidudu/publication/236123091_Diarrhea-Case-definition-and-guidelines-for-collection-analysis-and-presentation-of-immunization-safety-data_2011_Vaccine/data/02e7e51630c15e144e000000/Diarrhea-Case-definition-and-guidelines-for-collection-analysis-and-presentation-of-immunization-safety-data-2011-Vaccine.pdf (accessed October 25, 2023).
- [63] A. Agunu, S. Yusuf, G.O. Andrew, A.U. Zezi, E.M. Abdurahman, Evaluation of five medicinal plants used in diarrhoea treatment in Nigeria, *J. Ethnopharmacol.* 101 (2005) 27–30. <https://www.sciencedirect.com/science/article/pii/S0378874105002643>. (Accessed 25 October 2023).
- [64] J. Hu, W.-Y. Gao, N.-S. Ling, C.-X. Liu, Antidiarrhoeal and intestinal motulatory activities of Wei-Chang-An-Wan extract, *J. Ethnopharmacol.* 125 (2009) 450–455. <https://www.sciencedirect.com/science/article/pii/S0378874109004450>. (Accessed 25 October 2023).
- [65] A.B. Awad, J. Toczek, C.S. Fink, Phytosterols decrease prostaglandin release in cultured P388D1/MAB macrophages, *Prostagl. Leukot. Essent. Fat. Acids* 70 (2004) 511–520. <https://www.sciencedirect.com/science/article/pii/S0952327803002412>. (Accessed 25 October 2023).
- [66] K.Z. Long, J.L. Rosado, W. Fawzi, The comparative impact of iron, the B-complex vitamins, vitamins C and E, and selenium on diarrheal pathogen outcomes relative to the impact produced by vitamin A and zinc, *Nutr. Rev.* 65 (2007) 218–232, <https://doi.org/10.1111/j.1753-4887.2007.tb00299.x>.
- [67] R. Ponnulakshmi, B. Shyamaladevi, P. Vijayalakshmi, J. Selvaraj, *In silico* and *in vivo* analysis to identify the antidiabetic activity of beta sitosterol in adipose tissue of high fat diet and sucrose induced type-2 diabetic experimental rats, *Toxicol. Mech. Methods* 29 (2019) 276–290, <https://doi.org/10.1080/15376516.2018.1545815>.
- [68] L.A. Usman, O.S. Oguntoye, R.O. Ismael, L.A. Usman, O.S. Oguntoye, R.O. Ismael, PHYTOCHEMICAL PROFILE, ANTIOXIDANT AND ANTIDIABETIC POTENTIAL OF ESSENTIAL OIL FROM FRESH AND DRIED LEAVES OF *Eucalyptus globulus*, *J. Chil. Chem. Soc.* 67 (2022) 5453–5461, <https://doi.org/10.4067/S0717-97072022000105453>.
- [69] G. Alper, M. Olukman, S. İrer, O. Çağlayan, E. Duman, C. Yılmaz, S. Ülker, Effect of vitamin E and C supplementation combined with oral antidiabetic therapy on the endothelial dysfunction in the neonatally streptozotocin injected diabetic rat, *Diabetes Metabol. Res. Rev.* 22 (2006) 190–197, <https://doi.org/10.1002/dmrr.586>.
- [70] S.A. Nirmal, S.C. Pal, S.C. Mandal, A.N. Patil, Analgesic and anti-inflammatory activity of β -sitosterol isolated from *Nyctanthes arbortristis* leaves, *Inflammopharmacology* 20 (2012) 219–224, <https://doi.org/10.1007/s10787-011-0110-8>.
- [71] C.C. Santos, M.S. Salvadori, V.G. Mota, L.M. Costa, A.A.C. de Almeida, G.A.L. de Oliveira, J.P. Costa, D.P. de Sousa, R.M. de Freitas, R.N. de Almeida, Antinociceptive and antioxidant activities of phytol *in vivo* and *in vitro* models, *Neurosci. J.* 2013 (2013). <https://downloads.hindawi.com/archive/2013/949452.pdf> (accessed October 26, 2023).
- [72] J. Ongko, J.V. Setiawan, A.G. Feronytha, A. Juliana, A. Effraim, M. Wahjudi, Y. Antonius, *In-silico* screening of inhibitor on protein epidermal growth factor receptor (EGFR), in: IOP Conference Series: Earth and Environmental Science, IOP Publishing, 2022 012075.
- [73] S. Kodidela, S.C. Pradhan, J. Muthukumaran, B. Dubashi, T. Santos-Silva, D. Basu, Genotype distribution of dihydrofolatereductase variants and their role in disease susceptibility to acute lymphoblastic leukemia in Indian population: an experimental and computational analysis, *J. Leuk* 4 (2016) 2.
- [74] R.A. Simmons, Cell glucose transport and glucose handling during fetal and neonatal development, in: *Fetal and Neonatal Physiology*, Elsevier, 2017, pp. 428–435.
- [75] J. Pannemans, M. Corsetti, Opioid receptors in the GI tract: targets for treatment of both diarrhea and constipation in functional bowel disorders? *Curr. Opin. Pharmacol.* 43 (2018) 53–58.
- [76] F. Camu, L. Shi, C. Vanlersberghe, The role of COX-2 inhibitors in pain modulation, *Drugs* 63 (Suppl 1) (2003) 1–7, <https://doi.org/10.2165/00003495-200363001-00002>.